LBL-22349
UC-28

Lawrence Berkeley Laboratory

UNIVERSITY OF CALIFORNIA

RECEIVED
LAWRENCE
BERKELEY LABORATORY

DEC 23 1986

LIBRARY AND
DOCUMENTS SECTION

Accelerator & Fusion Research Division

HEAVY ION FUSION ACCELERATOR RESEARCH (HIFAR)
YEAR-END REPORT: April 1, 1986–September 30, 1986

Heavy Ion Fusion Staff

October 1986

TWO-WEEK LOAN COPY

This is a Library Circulating Copy which may be borrowed for two weeks.

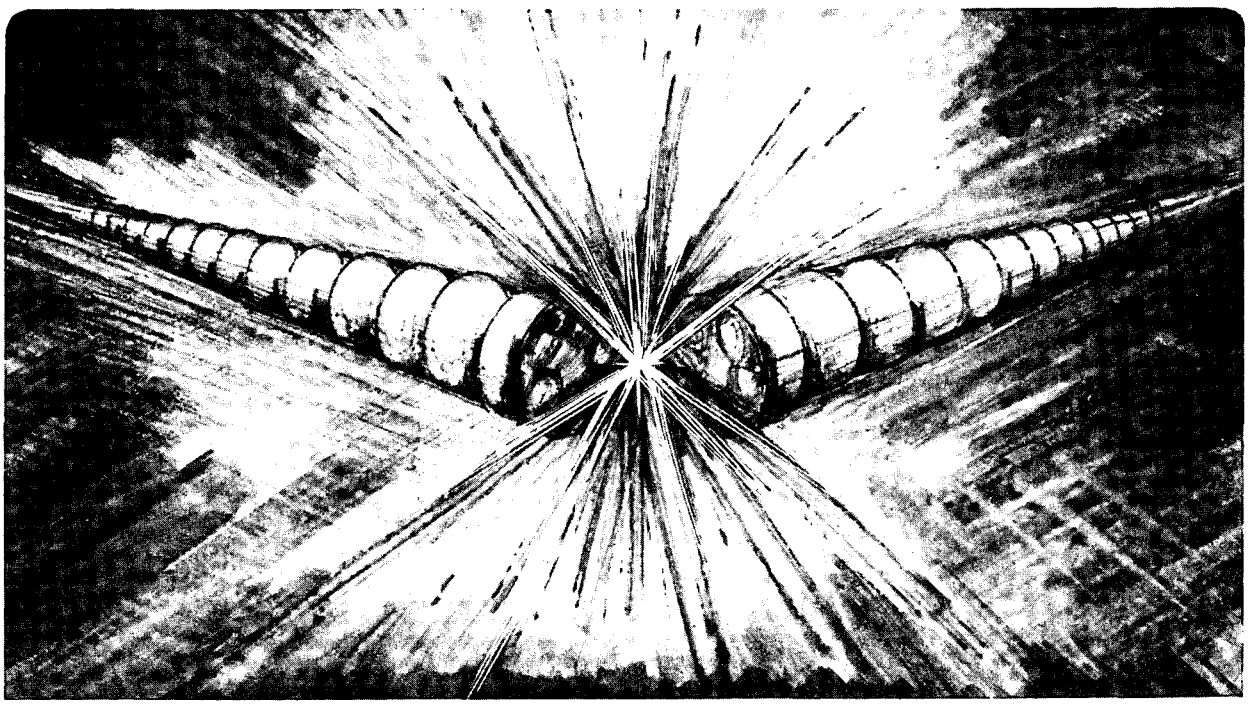

Prepared for the U.S. Department of Energy under Contract DE-AC03-76SF00098

LBL-22349 c.2

DISCLAIMER

This document was prepared as an account of work sponsored by the United States Government. While this document is believed to contain correct information, neither the United States Government nor any agency thereof, nor the Regents of the University of California, nor any of their employees, makes any warranty, express or implied, or assumes any legal responsibility for the accuracy, completeness, or usefulness of any information, apparatus, product, or process disclosed, or represents that its use would not infringe privately owned rights. Reference herein to any specific commercial product, process, or service by its trade name, trademark, manufacturer, or otherwise, does not necessarily constitute or imply its endorsement, recommendation, or favoring by the United States Government or any agency thereof, or the Regents of the University of California. The views and opinions of authors expressed herein do not necessarily state or reflect those of the United States Government or any agency thereof or the Regents of the University of California.

LBL-22349
HIFAN-350

HEAVY ION FUSION ACCELERATOR RESEARCH (HIFAR) YEAR-END REPORT*

April 1, 1986 - September 30, 1986

Heavy Ion Fusion Staff

Accelerator and Fusion Research

Lawrence Berkeley Laboratory
University of California
Berkeley, CA 94720

October 1986

Attention: This document is provided for DOE "Official Use". Distribution to other interested parties is made with the understanding that no information or experimental results given herein will be quoted without first obtaining the authors' permission, or until such information or results have appeared in the open literature.

*This work was supported by the Office of Energy Research, Office of Basic Energy Sciences, U.S. Department of Energy under Contract No. DE-AC03-76SF00098.

FOREWORD

The basic objective of the Heavy Ion Fusion Accelerator Research (HIFAR) program is to assess the suitability of heavy ion beam accelerators as igniters for Inertial Confinement Fusion (ICF). A specific accelerator technology, the induction linac, has been studied at the Lawrence Berkeley Laboratory and has reached the point at which its viability for ICF applications can be assessed over the next few years.

The HIFAR program addresses the generation of high-power, high-brightness beams of heavy ions, the understanding of the scaling laws in this novel physics regime, and the validation of new accelerator strategies to cut costs. Key elements to be addressed include: 1) Beam quality limits set by transverse and longitudinal beam physics; 2) Development of induction accelerating modules, and multiple beam hardware, at affordable costs; 3) Acceleration of multiple beams with current amplification -- both new features in a linac -- without significant dilution of the optical quality of the beams; 4) Final bunching, transport, and accurate focussing on a small target.

TABLE OF CONTENTS

	Page
HIGHLIGHTS	1
MBE-4: MECHANICAL ASPECTS	5
MBE-4: QUADRUPOLE INSULATOR PERFORMANCE	6
MBE-4 PULSERS	7
120 kV PULSERS	8
MBE-4 EXPERIMENTAL PROGRESS	9
ACCELERATING VOLTAGE ERRORS IN MBE-4	10
IMPROVEMENTS TO THE COMPUTER CODE SLID	11
AUTOMATED ENERGY MEASUREMENT OF THE MBE-4 BEAMS	12
EMITTANCE GROWTH OF SPACE-CHARGE DOMINATED ION BEAMS DUE TO MIS-MATCH	13
PRELIMINARY DESIGN OF A $\approx$ 10 MV ION ACCELERATOR FOR HIF RESEARCH	14
STUDIES OF COMBINING BEAMS TRANSVERSELY	15
COMPUTER SIMULATION OF TRANSVERSE MIXING OF COMBINED BEAMS	16
ANALYSIS OF THE LOW VOLTAGE REGION OF AN HIF DRIVER	17
PUBLICATIONS AND INTERNAL NOTES	18

Page

HIF STAFF ROSTER 26

DISTRIBUTION LIST 27

HIGHLIGHTS

D. Keefe

1. By far the biggest activity of the HIFAR group has been centered on MBE-4, the four-beam proof-of-principle ion induction linac with the capability of beam-current amplification. By the end of the year, 12 of the 24 accelerating units and 4 of the 6 transport sections were in place. Each accelerating unit contains many cores driven by two or more pulsers. An increase in beam-current by a factor of 2.5 was recorded, and a smooth current wave-form has been achieved by carefully tuning the accelerating voltage waveforms.

2. As expected, the design, fabrication, and tuning of the pulsers to drive the induction cores has involved considerable effort which has paid off in valuable experience in solving the relevant problems. Successful computer-modeling of the non-linear behavior of the cores has now been achieved. Determining the correct settings for the timing and the wave-forms of the pulsers has been accomplished by turning on each of the pulsers sequentially and observing the beam-current profile some distance downstream. The amplitude and timing of each pulsers can be adjusted to bring the current profile as close as possible to the desired shape.

3. The computer code, SLID -- due to C. Kim -- has proved a powerful tool in understanding the longitudinal beam dynamics in MBE-4. SLID is especially important for calculating the trim fields (so-called "ears") that prevent the ends of the bunch from spreading due to space-charge. The needed fields are related to the gradient in line-charge density by a geometry factor, g, which has been calculated for our case by L. Smith. It has been possible to determine g

experimentally in MBE-4 by careful measurements of the beam current and beam energy profiles and a comparison with SLID calculations; the results agree with the Smith prediction. The SLID code has now been upgraded to include the non-zero transit-time across the accelerating gaps.

4. To our surprise, a succession of tiny vacuum leaks has steadily occurred at the base of the Re-X insulators in the voltage feed-throughs to the electrostatic quadrupoles. These insulators are being replaced with Pyrex insulators which are quite satisfactory. In the spirit of an R and D program, however, we are investigating into the cause of the failure. One speculation, at the moment, is that the doubly-curved section of the metal spinning embedded in the end of the Re-X was formed with inadequate heat-treatment and has become porous through cycling of the MBE-4 vacuum system.

5. Some months ago we learned that a project to build an electron induction linac by Ford Laboratories had been discontinued. We then purchased enough of their fabricated silicon-steel cores to complete MBE-4, and embarked on a study of their pulser design to see if their excess pulsers could be usefully incorporated in MBE-4. This, indeed, proved to be the case but at the cost of modifications to the planned accelerating schedule in the last half of MBE-4. It was pleasing to find that the induction linac design proved flexible enough to accommodate a rather different core arrangement, and quite a different pulser design. The incorporation of the new pulsers, switched by spark-gaps rather than thyrations, gives a broader base to our pulser technology development.

6. High precision in the measurement of the beam properties in MBE-4 has been a major aim. The computer-controlled emittance scanning system developed for

the previous Single Beam Transport Experiment (SBTE) is in use in MBE-4 and relieves much of the tedium of carrying out the rather lengthy emittance scans. Computer-control has now been extended to the energy-analyzer diagnostics with corresponding benefits.

7. High-current, low-emittance beams are especially susceptible to emittance growth because non-linearities in the transverse space-charge fields can rapidly impart added transverse velocities to the beam particles. Whether beams that are not matched to the transport lattice (i.e., beam properties that are not strictly periodic with the lattice period) are subject to emittance growth has been the subject of speculation but not much detailed study. Two modes occur for the envelope oscillations of the beam in a transport lattice -- symmetric (monopole, sausage) in which $\Delta x = \Delta y$, and antisymmetric (quadrupole) in which $\Delta x = -\Delta y$. A preliminary set of experiments with the SBTE gave the interesting result that the emittance growth could be large for a purely antisymmetric mismatch mode but absent for the symmetric mode.

8. In this period, a program plan, "Heavy Ion Fusion Accelerator Research: An Outline Plan" (PUB-5178), was developed to address the needs for CY88 through CY92. A cornerstone of the plan is the assembly of a multibeam accelerator experiment of significantly higher voltage (10 MV) than MBE-4, in which ions with higher speed could be focussed and bent with magnetic fields. Such an experiment can test, in a scaled way, the remaining several features needed for a driver, which still remain addressed only on paper. Because it would encompass all the beam-manipulation systems needed in an ICF driver it was designated ILSE, for Induction Linac Systems Experiment.

9. Since a cost-saving feature in a driver is the use of a large number of beams early on (e.g. 64), which are later combined to a smaller number (e.g. 16), the present ILSE concept models this operation by starting with 16 beams and combining them to produce 4. Some hardware design concepts have been developed for the method of bringing four separated beams into close proximity and then launching them into a single transport channel. At the point of union, the space-charge distribution is non-uniform resulting in non-linear space charge fields which lead to emittance growth above and beyond the purely geometric factor (c.f.. #7, above). How this extra emittance growth depends on the configuration of the beams as they unite is the subject of an intensive PIC simulation study.

10. The LBL computer code LIACEP (for Linear Induction Accelerator Cost Evaluation Program) has been extensively used for the past two years in the Heavy Ion Fusion Systems Assessment (HIFSA) activity. Originally, the primary intent of the program was to use minimum cost as a constraint to determine the balance between the space devoted to transport elements and that used for acceleration units, at each point along a driver. Recognized inadequacies in the code at the very lowest energies were of no consequence in the HIFSA application. However, for quite small systems (such as ILSE), which are more appropriate to the immediate future of HIFAR, these deficiencies can result in misleading answers. A systematic effort is under way to discover and correct all the defects peculiar to the low energy part of the linac design code.

11. HIFAR staff have presented papers at a total of eleven conferences in the past six months (not the least of which was the International HIF Symposium in Washington, DC, in May, 1986). This represented an unprecedented hectic activity in this period.

MBE-4: MECHANICAL ASPECTS

D. Vanecek and R. Hipple

The MBE-4 Heavy Ion Fusion Program is on schedule as described in the program plan, Feb. 1985 [1]. The four cesium ion beams are now transported through Section D, the Induction Cores are installed through Section C, and a full complement of Diagnostics are operational through Section D. The above items are shown diagrammatically in Fig. 1 and photographically in Fig. 2.

The problems that arose with the assembly of the Section C transport column (see Half-Year Report, 1986) have been solved and the column was succesfully assembled and Sections C and D were installed in August 1986. The four Cesium Ion Beams have now been transported through to Section D. Section E is now being fabricated.

The Induction Core Modules for Section C are shown in Fig. 3. The individual core packages are packaged similar to those used in Section B. They contain Astron Cores, 1.4-inch wide Silicon Cores, and 4.0-inch wide Silicon Cores. All the Cores are wound with .002 inch thick ribbon. For the details of the individual core packages, see Half-Year Report for FY86, page 4, Fig. 3. The Induction Core Modules for Section D are in design at this time and it appears as though this Section will be quite different from the previous three sections. This change will be discussed in future reports.

The MBE-4 accelerator has the following diagnostics: 3 sets (vertical and horizontal) of Harps, 3 sets (vertical and horizontal) of Emittance Slits, 5 Faraday Cups, one Aperture Plate, and one Mirror Probe. The above diagnostics may be placed in any port in the diagnostics boxes to enable the experimentalist to diagnose all the four beams. See Fig. 1 for the present arrangement of the diagnostics.

The high voltage feed-thru insulators that power the electrostatic quadrupoles, (see Fig. 4) have developed a vacuum leak. These insulators were vacuum tight (10^{-9} Torr range) before installation, but over a short period of time they developed a vacuum leak (10^{-6} range). The leaks occur around the metal tube that extends from the glass insulator (see Fig. 4A). These leaks appear in 3 places; the bending radius of the tube, along the metal-to-glass seal, and the weld area. One of the suspected reasons for this vacuum failure is fatigue of the metal tube due to the cycling of the vacuum system. We are now in the process of replacing these insulators. This insulator is similar to the one now being used on the Single Beam Transport System where it performed very successfully. The mounting of the present Re-X insulator will be redesigned after we have determined the exact reason for failure.

The induction insulator (see Fig. 4) that is used between the Quadrupole Doublets has not developed this problem, and should not because of the way it is mounted.

Reference

1. "Program Plan for the MBE-4 Multiple Beam Experiment," LBL Report No. 19592 (Feb. 1985).

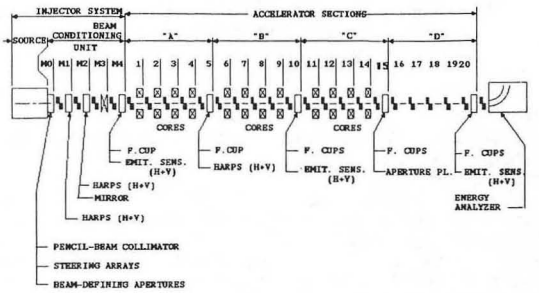

XBL 8611-4347

Fig. 1. Diagram illustrating the components installed and operating on the MBE-4 apparatus at the end of August 1986.

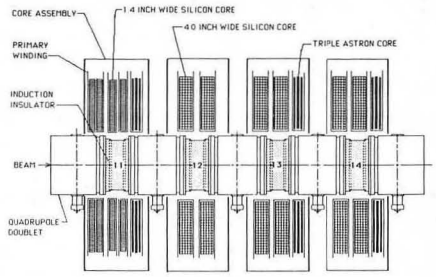

XBL 8611-4348

Fig. 3. Arrangement of cores for accelerator Section C.

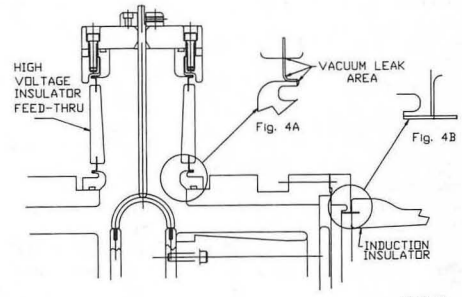

XBL 8611-4349

Fig. 4. Diagram showing the electrostatic quadrupole doublet assembly; the high voltage feed-thru insulator; and the induction insulator.

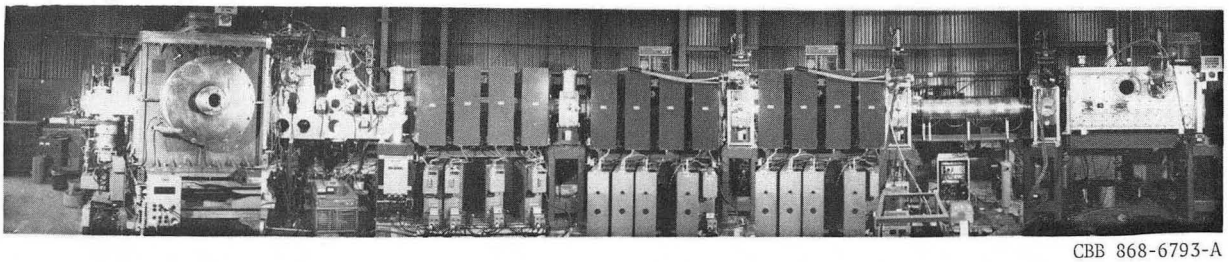

CBB 868-6793-A

Fig. 2. Photo of the MBE-4 apparatus September 1986 showing (from left to right): the large tank containing the four-beam source and its pulser; the diagnostic boxes and isolation valve of the Bean Conditioning Unit; the diagnostic box and the four square housings containing the induction acceleration cores with the induction pulsers located underneath for accelerator Section A, B, and C; the diagnostic box and the beam transport apparatus for accelerator Section D; and finally the large tank containing the energy analyzer.

MBE-4: QUADRUPOLE INSULATOR PERFORMANCE

C. Pike, R. Hipple, G. Stoker, and D. Vanecek

Certain experiments with the MBE-4 experiment to test beam performance with very large velocity shear required quadrupole voltages in Sections "A" and "B" to be larger than in the original design schedule.

We were surprised to find difficulties in achieving the desired voltages, namely that the voltage holding ability had become degraded. Measurements in June, 1986, indicated that, while some quadrupoles could be conditioned back to their initial voltage values of 40 kV, the majority were limited to less than 34 kV [1]. See Fig. 1 for details. To understand why, we embarked on a fresh evaluation of the two key insulators -- the Re-X high voltage feed-through, and the steatite stand-off insulators between the opposite-polarity quadrupole electrodes. In addition, we tested some other insulator types and the data are summarized here. Meanwhile, the cause of the degradation was traced to small gas leaks in the metal embedments in the Re-X feedthroughs, as reported in "MBE-4: Mechanical Aspects", elsewhere in this report, where a sketch of the arrangement is shown.

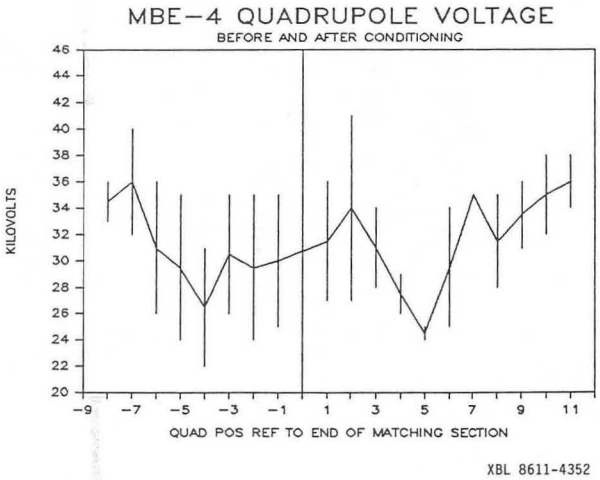

Fig. 1.

The quadrupole feed-through insulators were again tested in our evacuated test stand. The type of insulator being used, Re-X™, tested to 50 to 55 kV and should have worked well at 30 kV. It will not, however, be suitable for Sections "D", "E", and "F", where the quadrupole voltages increase and could be as high as 80 kV in Section "F". Hence, we have been testing pieces of Pyrex™ caustic waste drain pipe similar to the type of quadrupole feed-through insulators used in the SBTE. Two types were tested, the first being six inches long and the other twelve inches long. These last tests were encouraging since voltages well above the required 80 kV could be achieved with the twelve-inch unit.

Since we had no reason to suspect the feed-through insulator at this point our attention turned to the quadrupole stand-off insulators.

STEATITE INSULATORS: These insulators were retested as defined in HIFAR-60 [2]. The results were consistent with the previous tests and should have worked well at 30 to 36 kV, but would not satisfy the requirements of Sections "D", "E", and "F" $V_f = 80$ kV as stated above. We know that 85% Alumina would work in these sections, but decided to do further testing of a subdivided Steatite insulator.

Subdividing and grading insulators should raise their voltage-holding ability but could cause problems with the alignment of the quadrupole structure since the length of these insulators is a critical factor in the alignment. R. Hipple suggested putting an O-Ring around the insulator at the center. Where previously the turn-on voltage (after the first spark) was about 30 kV, this time it was 75 kV and conditioned up to 120 kV in about five hours (see Table 1). Instead of an O-ring at the center-point, a plated band of metal was tried (nickel on copper) on another Steatite insulator. Turn-on was now lowered to 65 kV and the maximum voltage held was 120 kV (Table 1). Two bands of metal, equally spaced, resulted in an even lower turn-on of 55 kV and an upper limit of 105 kV (Table 1). All of these modifications, however, resulted in higher turn-on and operating voltages than were achieved with an unmodified insulator.

Table 1: CONDITIONING CHARACTERISTICS

	Bare	"O" Ring	1 Band	3 Bands
STEATITE				
1st Spark	30 kV	75 kV	65 kV	55 kV
Conditioned	65 kV	120 kV	120 kV	105 kV
85% ALUMINA				
1st Spark	50 kV	75 kV	N/A	N/A
Conditioned	125 kV	145 kV	N/A	N/A

85% ALUMINA INSULATORS: These insulators were also tested as defined in HIFAR-60 and again the results were consistent. With the bare insulator the turn-on voltage was 50 kV and the maximum achieved was 125 kV after conditioning. A sample with an O-ring also showed improved performance; it turned on at 75 kV and reached 145 kV in less than five hours.

CONCLUSIONS: It was clear that electrically the feed-through insulators were not the culprit nor was the quadrupole insulator itself. Careful leak checking revealed tiny leaks in the metal embedment around the base of the Re-X™ feed-through insulators. Further inspection revealed small cracks in the formed metal which was the interface between the insulator and the mounting flange. Speculation is that this material cracked at flaws in the metal since it was deformed each time the system was evacuated and then expanded when the system was vented. Therefore, the problem was not evident from any testing that had been done on the test stand because these units were not cycled until they failed, but only a few times at the most.

The quadrupole insulator O-Ring phenomenon is not yet fully understood. It is evident that the plated rings or bands being only about one (1) mil thick will cause voltage enhancement at their sharp edges but they still work, most probably by modifying the location of the equipotential lines.

References

1. C. Pike and J. Stoker, "MBE-4 Quad Insulators - Voltage Holding after Exposure to Beam," HIFAR Note-76.

2. C. Pike and J. Stoker, "MBE-4 Insulator Tests," HIFAR Note-60.

MBE-4 PULSERS

D.E. Gough and D. Brodzik

Pulsers are now operational on the four acceleration gaps of section B of MBE-4 whilst those for the four gaps of section C are currently being installed. The accelerating voltages at the gaps of section B consist of a composite of capacitor discharge and (1-cos ωt) waveforms using a combination of 1.4" silicon steel cores capable of 24 mVs/core and 0.5" nickel-iron cores capable of 6.8 mVs/core.

The rise time of the capacitor discharge pulsers at the first three gaps of section B have been adjusted so that the voltage generated will control the longitudinal beam spread at the head of the beam as well as the imperfection in the source. The fourth gap of section B includes a trim pulser which controls the longitudinal beam spread at the tail of the beam.

Each gap voltage is a composite of at least two pulsers. Since their voltage waveforms are adjustable in amplitude up to 25 kV together with trigger time having a resolution of 10 nsec it is possible to provide a wide range of accelerating voltage waveform shapes. Fine tuning of the pulsers at a given gap are carried out in conjunction with experimental data taken using the previously set accelerating voltages.

Computer modelling was again used to predict the performance of the pulsers. Measurements were made at different charge voltages for the core packages being used to assist in core modelling. Data for a core package containing two 1.4" silicon steel cores at different charge voltages using a capacitor discharge pulser is shown at Fig. 1, the initial resistance value being used to provide a simple equivalence of the core package. A better approximation than this is a resistor in parallel with an inductance to represent the core inductance; a series inductance is used to represent the leakage inductance of the core. The pulser model is completed by the addition of a series inductance and resistance between the core and source to represent the cable inductance, which can be lumped together with the core leakage inductance, and the voltage source resistance. This computer model with the values used are as shown at Fig. 2. The calculated and measured pulser characteristics for a core package containing two 1.4" silicon steel cores and a capacitor discharge pulser at different charge voltages are shown at Figs. 3 and 4 respectively.

The pulsers being installed at the four accelerating gaps of section C are modelled in a similar manner to that outlined previously. Additional silicon steel cores which are 4" wide and capable of some 60 mVs/core had become available and are used in conjunction with some of the existing cores. Once again each accelerating gap voltage is a composite of at least two pulsers.

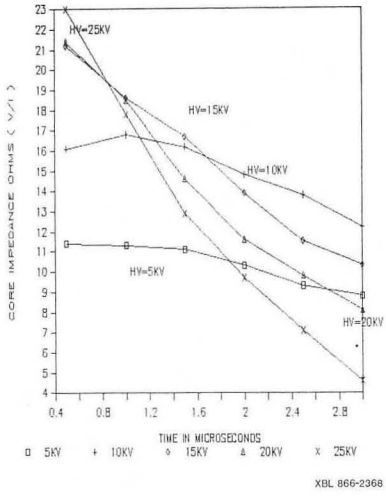

Fig. 1. Measured values of core impedance with time for a core package containing two 1.4" silicon steel cores for the capacitor discharge pulser at different charge voltages.

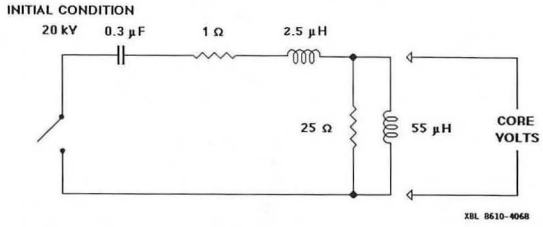

Fig. 2. Computer model of a capacitor discharge pulser at a charge voltage of 20 kV using a core package containing two 1.4" silicon steel cores.

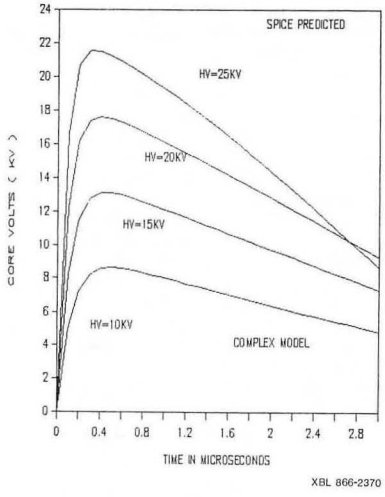

Fig. 3. SPICE predicted core voltage for a core package containing two 1.4" silicon steel cores and a capacitor discharge pulser at different charge voltages.

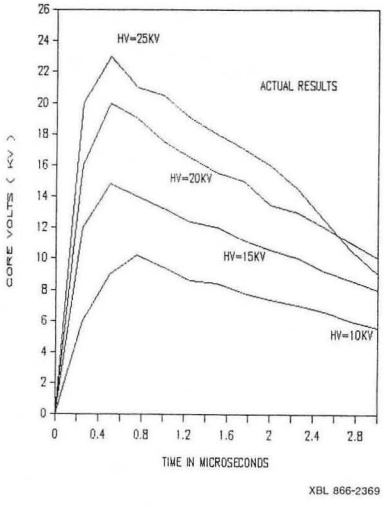

Fig. 4. Measured core voltage for a core package containing two 1.4" silicon steel cores and a capacitor discharge pulser at different charge voltages.

120 kV PULSERS

Andy Faltens, Chet Pike and Jerry Stoker

During August, 1986, we tested a spark gap switched pulser that was a spark gap switch borrowed from Ford Laboratories of Dublin, CA. These pulsers had been intended for powering the induction cores of an electron induction accelerator which was partially constructed but never completed, and from which we had already purchased some induction cores for use in finishing MBE-4. The tests were intended to evaluate whether the technology appeared suitable for the future ILSE, and whether it could be applied to the remainder of MBE-4 to perhaps reduce costs and complexity, and also to enable us to explore a different technological approach. These preliminary tests showed that the cores could probably be driven to 30 kV each for 1.5 μsec, enabling one core to supply the bulk of the required voltage across one gap. The initial design of MBE-4 had been based on a flat 30 kV pulse across every gap in the higher energy portions of the machine, and it appeared that with some waveform correction with separate, lower powered pulsers, the Ford pulsers could be adapted to our requirements. With further tests and some circuit modifications, we were able to drive four induction cores with one pulser, thereby supplying most of the voltage for a four gap section.

The specific prototype which we have been concentrating on and are still developing requires a minor reconfiguration of the acceleration schedule. In the new design, the 30-30-30-30 kV acceleration sequence is changed to 0-60-60-0 for the main pulsers, with trim pulsers being used in place of the 0's as required. With this change, the voltage pulse is just long enough to span the bunch duration and the beam transit time between two adjacent gaps. Each gap is powered by two induction cores in a series connected configuration, and the two pairs of cores are driven in parallel by one pulser, as shown in Fig. 1. Because some of the accelerator components will be operating at about twice their initial design voltages, some voltage upgrading of the components will be required. The acceleration gap itself has withstood the 60 kV pulse, the induction cores have withstood the 30 kV pulses to which they are exposed, but the interconnecting cables will probably have to be upgraded.

A part of the recent development was the spark gap triggering system. The existing trigger pulsers, a single stage spark gap and a three stage Marx generator, each put out a short pulse with about a 20 ns risetime and 60 ns duration. These short pulses would trigger the main gap for a few hundred pulses, after which triggering would become erratic. Recently we tried several modifications of the spark gap, of which the last one is the incorporation of a corona source within the spark gap envelope to supply a small amount of preionization, which have greatly reduced the erratic performance.

Based on these several favorable results, we have begun the layout of the entire system, with the goal of installing it in the MBE-4 accelerator in the next few months.

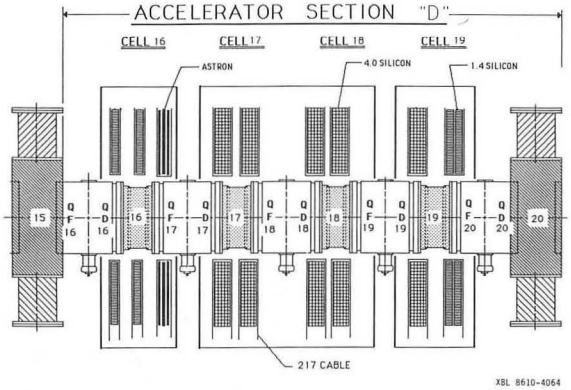

Fig. 1a. Physical layout of the induction cores for sections D,E, and F. The four central cores are powered by one pulser to provide 120 kV acceleration total, at 60 kV per gap.

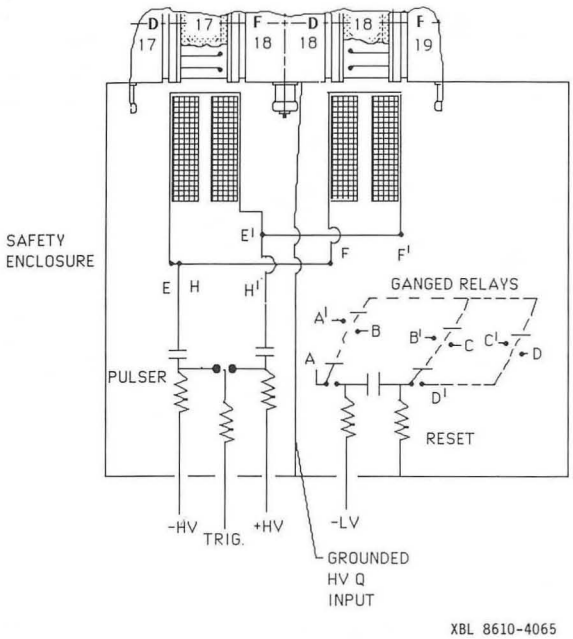

Fig. 1b. Schematic diagram of the electrical connections for use with the 120 kV pulser

MBE-4 EXPERIMENTAL PROGRESS

A.I. Warwick,† T.J. Fessenden, C.H. Kim

The Multiple Beam Experiment, MBE-4, will consist of six sections (A-F) each containing four accelerating units. Experiments have been proceeding one section at a time as the apparatus is built. In April and May, MBE-4 consisted of the injector, matching section, accelerating sections A and B, and the energy analyzer.

Because the longitudinal space charge forces must be carefully compensated by the accelerating waveforms for proper operation of MBE-4, it is necessary to determine the degree to which they are reduced by the conductors that surround the beam. We performed an experiment to determine the correct geometrical factor g to be used in expression for the longitudinal space charge electric field E_z. This field is related to the beam parameters by

$$E_z = -g\ \partial\lambda/\partial z \Big/ (4\pi\epsilon_0)$$

where λ is the line charge density of the beamlet and ϵ_0 is the free space permittivity. L. Smith has estimated that $g = 3.4$ for the geometry of MBE-4. Figure 1 shows the measured current and kinetic energy waveforms at the end of section B (gap 10) for a drifting beam. SLID code calculations using various values of g, which begin with the measured waveforms at the entrance to the accelerator are also shown. These data suggest that $g = 2.8\ (\pm\ 0.6)$.

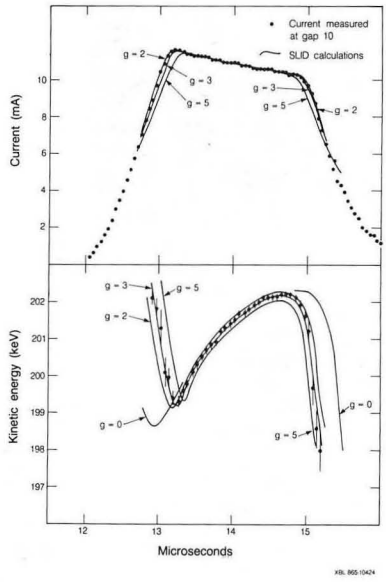

Fig. 1. Empirical determination of the longitudinal space charge factor g. Computations of the longitudinal dynamics of a drifting bunch through sections A and B for various values of g are compared with the measured kinetic energy and current waveforms at gap 10.

The waveforms and the beam energy versus time both with and without acceleration were measured and compared with predictions from the SLID code. Figure 2 shows the current and kinetic energy waveforms at gap 10 after acceleration. The dots are experimental measurements of the beam current using Faraday cups and of the beam energy from the energy analyzer obtained with a digitizing oscilloscope. These are to be compared with predictions of the SLID code that are based on measurements of the beam current and energy at the entrance to the accelerator and on measurements of the accelerating wave forms on each of the first eight accelerating gaps.

†Now at GSI Darmstadt, W. Germany.

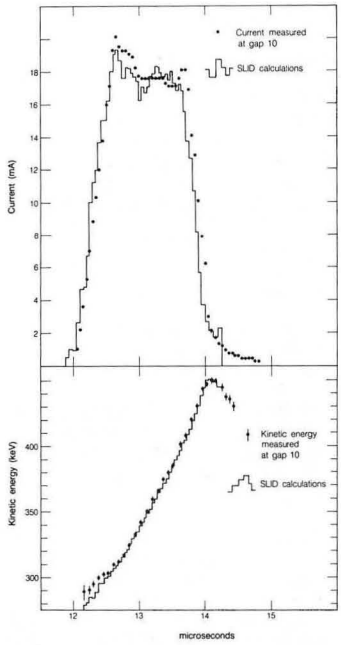

Fig. 2. Measured and calculated current and kinetic energy waveforms for the right beam at the end of section B. Current is amplified by a factor of 1.6.

Beam space charge tends to reduce rapid current fluctuations as illustrated in Fig. 3. The upper trace shows fluctuations on a 0.6 mA pencil beam with weak longitudinal space charge forces that was accelerated to station 10. The lower trace is the full current beam accelerated by the same voltages. The oscilloscope gains were adjusted so that relative comparisons could be made.

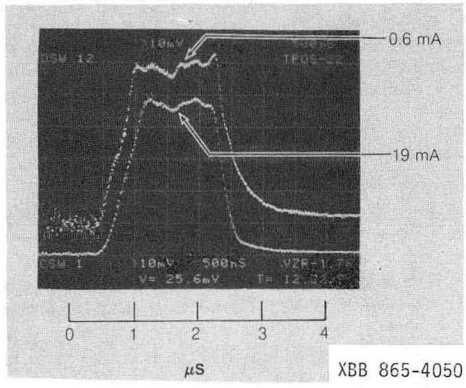

Fig. 3. Comparison of current modulations caused by small acceleration errors at the early gaps on a) a space-charge dominated 19 mA beam and b) a 0.6 mA beam with negligible self forces.

During April and May the current waveforms at the exit of Section B were as shown in Fig. 3. Accelerating voltage errors in the first few gaps rapidly turn into beam current fluctuations which grow with z. These were mostly eliminated by careful adjustment and compensation of the accelerating voltages as described by Kim [1] in this report.

Reference

1. C.H. Kim, "Accelerating Voltage in MBE-4," this report.

ACCELERATING VOLTAGE ERRORS IN MBE-4

C. Kim

Introduction

Accelerating voltage errors generate current modulations which could eventually turn into a longitudinal emittance growth. Systematic errors can be reduced to a desired level by correcting the voltage waveforms. By following a careful tuning procedure for the accelerating voltage waveforms, we were able to eliminate most of the systematic errors accumulated during the first 8 accelerating gaps of MBE-4 and obtain much smoother current-pulse shapes at cell 10 without any additional trim pulsers. Effects due to random errors are small but more difficult to correct.

Systematic Errors

The accelerating voltage waveforms in MBE-4 were originally designed such that the current-pulse shape at injection should be self-replicated in the subsequent accelerating gaps [1]. Our earlier experimental data [2] showed that self-replication was not working perfectly during the first 8 acceleration gaps because small voltage errors caused significant current modulations 5 to 10 gaps later. Most of these errors were systematic errors; the current modulations repeated pulse after pulse.

We were able to reduce most of these current modulations by carefully adjusting the accelerating voltage waveforms according to the following tuning procedure: The gap voltages were turned on sequentially starting from the first gap while the current pulse shape at the end of the linac (10-th cell) was monitored. The voltage waveform at each gap is synthesized with 2 to 3 pulsers. The amplitude and timing of each pulser for the gap were adjusted until the current shape at gap 10 reached a satisfactory level of smoothness. The injected and the final current-pulse shapes after the tuning are shown in Fig. 1 for all four beams. They show a significant improvement over our previous results reported at the 1986 HIF Symposium in Washington, DC [2].

The remaining small current modulations (still visible in Fig. 1) are due to kinetic energy errors on the order 100 eV. This corresponds to less than 1% of the typical gap voltage and less than 0.1% of the beam kinetic energy. In principle, these errors can be further corrected with additional trim pulsers. However, it may not be necessary to make any further corrections at this time because of a favorable scaling law for systematic errors discussed below. If the systematic errors are corrected to an accuracy of a few percent of the accelerating gap voltage, the fractional error of the beam kinetic energy decreases rapidly as the beam is accelerated.

When a high frequency correction has to be made, it has to be applied across a narrow gap in order to reduce the ion-transit-time effect. This effect is discussed elsewhere in this Report.

Random Errors

Random errors are mostly generated by pulser timing jitters (about 10 nano-seconds) and amplitude fluctuations. Waveforms were synthesized in such a way that the effect of these errors are minimized [1]. Current modulations due to random errors are about one order of magnitude smaller than the one due to systematic errors shown in Fig. 1. However, these errors are more difficult to correct and may be left to accumulate over the entire linac. Under these circumstances, the resulting longitudinal emittance growth is of great concern. We are planning to study these effects of random errors closely when more accelerating modules are added to MBE-4.

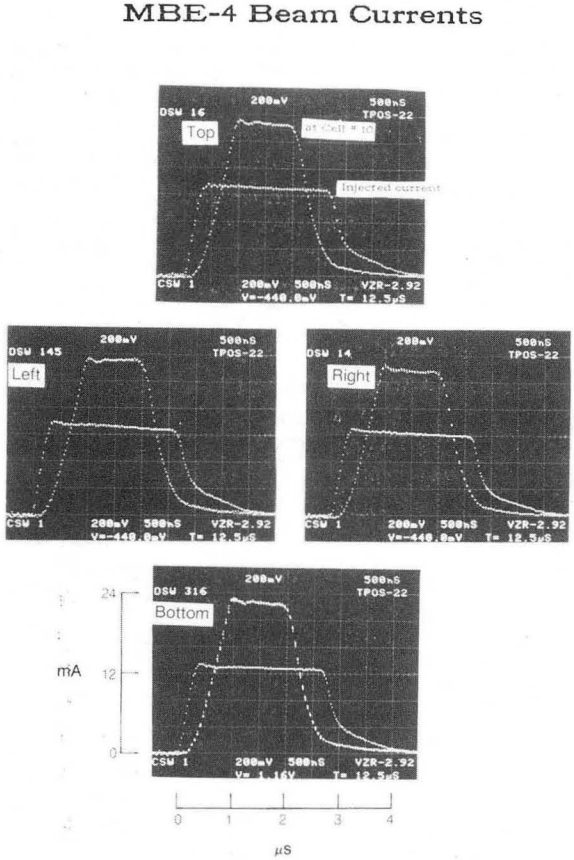

XBB 868-6643

Fig. 1. MBE-4 current-pulse shapes show effects of the systematic error of the accelerating voltages. All four beams at the injection point and at cell number 10 after tuning are shown. No additional trim pulsers were used.

References

1. C.H. Kim, V.O. Brady, T.J. Fessenden, D.L. Judd, and L.J. Laslett, IEEE Trans. Nucl. Sci., Vol NS-32, 3190(1985).

2. T.J. Fessenden, D.L. Judd, D. Keefe, C. Kim, L.J. Laslett, L. Smith, and A.I. Warwick, International Symposium on Heavy Ion Fusion, Washington, DC, May 27-29, 1986 (To be published).

IMPROVEMENTS TO THE COMPUTER CODE SLID

C. Kim

Introduction

The code SLID has been used to (1) design accelerating voltage waveforms for a given set of physics and technological requirements, (2) predict the energy- and the current-pulse shapes as functions of time at any location along the linac for a given experimental condition, (3) find possible improvements to the experimental conditions for a more desirable longitudinal performance. The code became an indispensible tool in operating MBE-4 and analyzing the data. We have made several improvements and are contemplating making several others. Some of them are discussed below.

Ion Transit-Time Effect

One of the problems we had was that the current-pulse shapes predicted by the code always had more high frequency fluctuations than the ones measured experimentally. We found that the finite ion-transit-time effect (ignored in the code) was the main reason for the discrepancy. Lloyd Smith considered the frequency response of beam to high frequency voltage errors in accelerator modules [1]. His calculation showed that the effective amplitude of the high frequency noise is reduced by a factor $\sin(\omega\tau/2)/(\omega\tau/2)$ where ω is the frequency of the noise and τ is the ion-transit-time across the gap.

In order to incorporate the transit time effect, we have Fourier-analyzed the measured voltage waveforms and reconstructed them using the frequency response factor described in the previous paragraph. Figure 1 shows a comparison between the experimentally measured current waveform and the ones predicted by the code with and without the transit-time-effect. The agreement is much better when the transit-time effects are included.

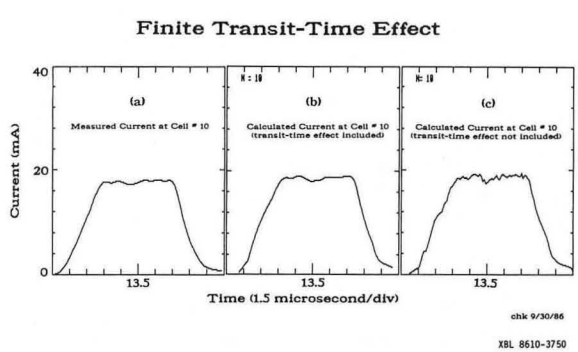

Fig. 1. A comparison between (a) the experimentally measured current waveform and the ones predicted by the code (b) with and (c) without the transit-time effect. The small dip in the middle of the bunch was caused by a voltage error in the second acceleration gap. This error was corrected later and the result is described elsewhere in this report.

The g-Factor

In the code, the longitudinal space charge forces are calculated by differentiating the line charge density and multiplying it by the g-factor. We measured the g-factor experimentally by comparing the measured and the predicted current waveforms (see Warwick et al., elsewhere in this Report [2]). The waveform shape near the bunch-ends where the erosion due to the space charge forces are particularly sensitive to the value of the g-factor. The measured value of g was 2.8 and, when three of the four beams were blocked, decreased by a factor of 10%. These results agree well with the theoretical prediction by Lloyd Smith [3]. These results were reported at the International HIF Symposium [4].

Limitations

The code uses a 1-D model and assumes a value of zero for the longitudinal emittance. In light of the good agreements that we are observing between experiments and the code predictions, one might conclude that the finite emittance effects and the 3-D effects are small in MBE-4 in its present configuration. However, accumulation of random voltage errors and uncorrected systematic voltage errors may lead to a considerable longitudinal emittance growth as we add more accelerating modules. The 3-D effects near the bunch ends make the situation more complicated. In order to study these phenomena, we need to modify the code as well as to improve the resolution of the energy analyzer.

We are also studying ways to generate necessary accelerating voltage waveforms which will modify the current pulse shape to a desirable shape.

References

1. Lloyd Smith, LBL HIF Group Report, HIFAR-Note-66 (1986).

2. A.I. Warwick, T.J. Fessenden, C.H. Kim, "MBE-4 Experimental Progress," this report.

3. Lloyd Smith, LBL HIF Group Report, HIFAR-Note-53 (1986).

4. T.J. Fessenden, D.L. Judd, D. Keefe, C. Kim, L.J. Laslett, L. Smith, and A.I. Warwick, International Symposium on Heavy Ion Fusion, Washington, DC, May 27-29, 1986.

AUTOMATED ENERGY MEASUREMENT OF THE MBE-4 BEAMS

S.H. McCreight and A.I. Warwick*

During the summer of FY86, a system was developed that automated the data acquisition for the energy analyzer on MBE-4. The electrostatic energy analyzer is described in reference [1]. The system uses an IBM PC micro-computer to automatically adjust the voltage on the analyzer plates, collect the experimental data from the analyzer, and plot the data for presentation. The system allows the data to be taken more rapidly, while reducing inaccuracies in the measurement.

A block diagram of the computerized system is presented in Fig. 1. The experimenter specifies the energy band that is to be scanned and the number of scans to be taken. The correct voltages corresponding to the energy levels, are calculated and reference voltages sent to the power supply which applies an approximately correct voltage (to within 10%) to the bending plates of the analyzer. After allowing the power supply to settle, a digital voltmeter measures the actual voltage on the bending plates to within 1%. The beam passing through the analyzer strikes the detector and is recorded on a digitizing oscilloscope. The area under the trace is proportional to the number of ions responsible for the signal. At each energy eight pulses are averaged and the resulting waveform is read into the computer. This process is repeated at each energy level and the data stored for reprocessing. Gathering data at each level takes nearly 1 minute so the average time for a measurement is approximately 30 minutes.

Figure 2 shows a typical output of a separate program which has been written to generate a three-dimensional display of the data gathered from the analyzer. The oscilloscope traces recorded at each energy level are displayed along a third axis at a displacement proportional to energy. These data were taken in mid August after the section C and D drift tubes had been installed and the analyzer was located at the end of section D. The accelerator pulsers were not on for this measurement. The average energy of the beam, for this particular measurement, is about 200 keV, i.e. a beam drifted from the injector.

Figure 3 shows a plot of mean energy versus time of the data shown in Fig. 2. This was obtained by computing the mean energies of the detected signals at fixed time which were then plotted as a function of time. The bars represent two standard deviations of each computation.

There are two main advantages to the automated system. The first is that the entire process is controlled by the computer. Thus the energy analyzer data is automatically gathered, analyzed and stored for future use. Moreover, the need for the operator to adjust the analyzer voltage for each of the typically 30 energy levels necessary for a measurement is eliminated. The second is that the time to take a full measurement is cut by more than 50%, allowing more measurements to be taken in one period.

*Now at GSI Darmstadt, W. Germany.

Reference

1. S.S. Rosenblum and A. Faltens, "Electrostatic Energy Analyzer," Heavy Ion Fusion Half Year Report, Oct. 1, 1984-Mar. 30, 1985, LBL Report No. 19501.

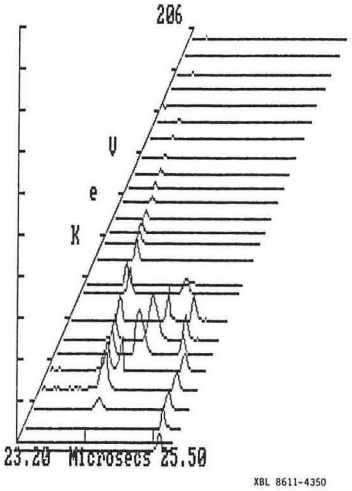

Fig. 2. 3-D plot of analyzer data.

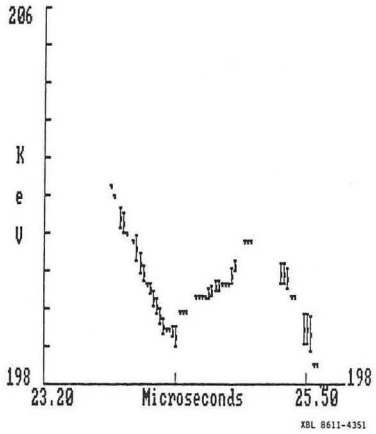

Fig. 3. Mean energy plot of data in Figure 2.

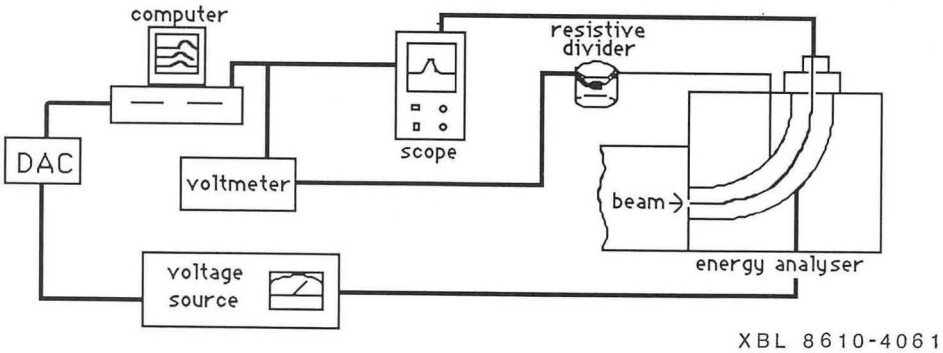

Fig. 1. Block diagram of the analyzer system.

EMITTANCE GROWTH OF SPACE-CHARGE DOMINATED IONS BEAMS DUE TO MIS-MATCH

M.G. Tiefenback and T.J. Fessenden

A practical consideration in the acceleration and transport of space-charge dominated ion beams for Heavy Ion Fusion is an evaluation of emittance growth resulting from beam mis-matches that may occur at transitions in the transport system through the accelerator. For tractability reasons most analytic approaches to beam mis-match have assumed that the beam was adequately described by a K-V distribution. This distribution is appropriate for a transport system that contains no non-linear effects. As a consequence, within such a theory, there is no possibility of phase-mix damping of mis-match oscillations.

To gain some experimental understanding of these phenomena we performed two experiments on the Single Beam Transport Experiment. In the first a beam with normalized emittance of $2\pi \times 10^{-7}$ m-rad was carefully matched to SBTE at a current of 9.5 mA (matched radius = 12.5 mm) and then attenuated with a transmission mask to 3.14 mA (matched radius = 8.9 mm) at Q1. As a consequence the mis-match oscillation was symmetrical. Figure 1 shows measurements of the rms beam size in the horizontal and vertical planes using "harps" at the accessible locations along SBTE. Also shown is the matched beam radius for a 3.14 mA beam calculated using simple envelope theory. After the attenuator, the beam envelope shows large excursions indicating a mis-matched beam. These damp as the beam passes through SBTE (nearly seven betatron periods) to a value near the matched beam radius. A measure of the emittance growth due to the apparent phase mix damping indicated no change in the beam emittance.

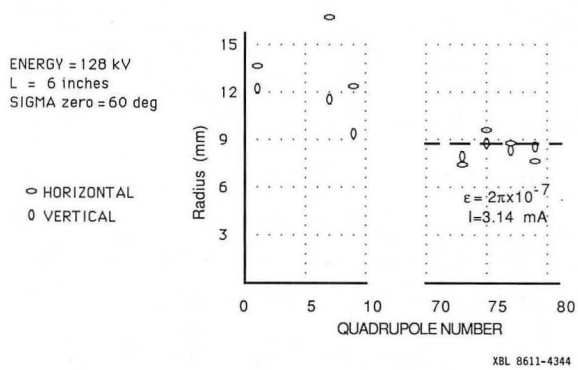

Fig. 1. RMS beam radius versus quadrupole location for a 9.5 mA beam that was attenuated to 3.14 mA at Q1.

Recently, a second beam matching experiment [1] was performed in which the mismatch was produced by adjustments of the quadrupole voltages in the matching section. The values were chosen with the aid of an envelope-equation computer code to excite either a symmetric or an antisymmetric envelope oscillation. The beam current used for these experiments was 4.6 mA and the beam emittance at the beginning of SBTE was $7 \times 10^{-8}\ \pi$ m-rad. Measurements of beam emittance at the end of SBTE (Q80) for an initially a) matched beam; b) symmetrically mis-matched beam; and c) antisymmetrically mis-matched beam are summarized in Table 1. The results of measurements of beam size of both a symmetrically and antisymmetrically mismatched beam are given in Fig. 2 and 3 respectively. The line in each figure is the expected beam radius calculated from simple envelope theory for the currents and emittances contained in Table 1.

Table 1
Increase in emittance of a 4.6 mA Cesium beam passing through SBTE.
The initial beam emittance was $7\pi \times 10^{-8}$ m-Rad.

Beam Fraction	Matched	Symmetric	Antisymmetric
100%	1.4	1.5	5.1
95%	1.0	1.0	4.2

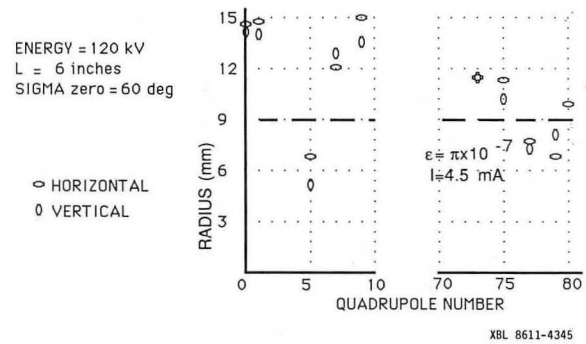

Fig. 2. RMS beam radius versus quadrupole location for a <u>symmetrically</u> mis-matched beam.

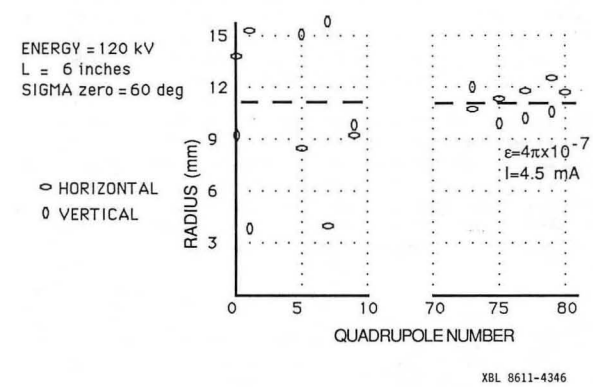

Fig. 3. RMS beam radius versus quadrupole location for an <u>antisymmetrically</u> mis-matched beam.

Phase space observations of the beam at the end of SBTE showed that, for the antisymmetric case, the beam had developed extensive tails that wrapped around the main distribution and reconnected. Phase space distributions for the symmetrically mis-matched beam were difficult to distinguish from those of an initially well matched beam.

These experiments indicate that in the SBTE at Cs^+ currents of 3-5 mA, both symmetric and antisymmetric mis-match oscillations damp by factors of 3-5 in just under seven coherent betatron periods at $\sigma_0 = 60°$. An initially antisymmetrically mis-matched beam shows significant emittance growth in passing through the experiment. An initially symmetrically mis-matched beam shows little to no emittance growth.

Reference

1. M.G. Tiefenback, HIFAR Note-92, August 18,1986.

PRELIMINARY DESIGN OF A ≈ 10 MV ION ACCELERATOR FOR HIF RESEARCH

Thomas J. Fessenden and Denis Keefe

We present the concept and a very preliminary physics design of an Induction Linac Systems Experiment, ILSE, that is intended to address many of the remaining accelerator physics issues that must be faced by an induction linac fusion driver. With data from this experiment we expect that the HIFAR program could complete its assessment of the induction linac as a practical heavy-ion driver for commercial inertial fusion power.

ILSE was designed to address: the physics of transversely combining space-charge dominated ion beams; the transition from an electrostatic to a magnetic beam transport system; the physics of bending ion beams with intense space charge and with time dependent energy; the physics of drift-compression current amplification; the focusing of intense ion beams to a 1-2 millimeter spot. In addition ILSE will advance the technology of heavy ion multiple-beam induction linacs much closer to that needed for a driver.

A block diagram of a conceptual design for ILSE is presented in Fig. 1. Sixteen beams of singly or doubly charged ions at 2 MV from the LANL injector [1] are matched to an electrostatic transport system and accelerated to 4 MV by a multiple beam induction accelerator with a pulse duration of one microsecond. At this point the beams are combined to four, and matched to a magnetically focused linac for further acceleration to 10 MV. Three of the beams are then blanked off and the remaining beam is deflected through a large angle (90 or 180 degrees) by a bending magnet and longitudinally compressed in a transport section. The beam is then used in final focus experiments. The length from the source to the end of the accelerator is approximately 50 meters.

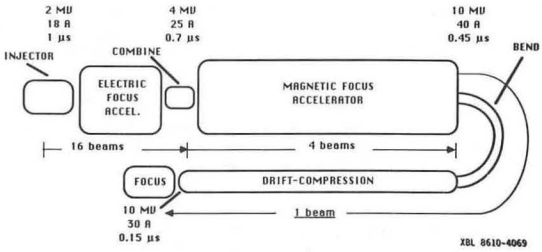

Fig. 1. Block Diagram of the ILSE Apparatus

A comparison of the parameters of the ILSE beams at the output of the accelerator with the parameters of MBE-4, and a fusion driver is presented in Table 1.

TABLE 1
Beam Parameters of MBE-4, ILSE, and a Driver

Parameter	MBE-4	ILSE	Driver
Ion	Cs^+	C^+ (AL^{++})	200^{+++}
Inj. Volt. (MV)	0.2	2	3
Final Volt. (MV)	1.0	10	3300
Final Current(A)	0.1	30	60000
Beam Energy (J)	0.1	125	3 MJ
Ion Velocity/c	0.004	0.04	0.3
Accel Grad. (MV/m)	0.07	0.22	0.5
# Beams	4	16-4	64-16
Pulse Width (μs)	2-1	1-0.5	24-.1
Charge (μCoul.)	0.1	15	900
Init. bunch length (m)	1.1	5.6	70
Final Perv. (Norm.)	3.8×10^{-4}	3.6×10^{-4}	5.6×10^{-5}

Figure 2 shows calculations of the beamlet current as a function of the beam energy for parametric focus electrode voltages and phase advance per period. Because the system must operate near the limit of the electrode voltages, bunch length shortening in this section of the accelerator is impractical. In these calculations the beamlet charge per meter is 0.2 μC/m which is approximately three times larger than that being used in the LANL injector development [1]. At constant bunch length (constant charge per meter), the current

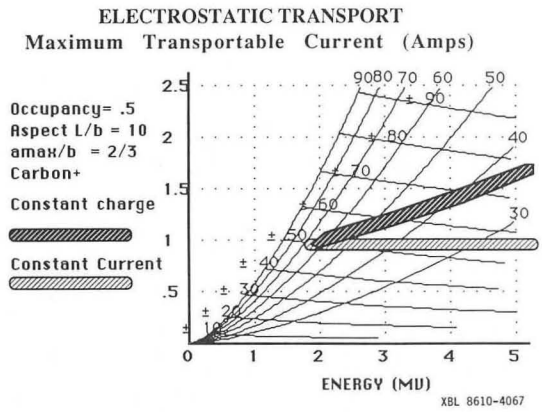

Fig. 2. Operating characteristics of the electrostatically focused accelerator. The parametric lines are at constant phase advance per period (σ_0) in degrees and at constant voltage from a quadrupole to the beamlet axis in kilovolts. (L = Half-period of lattice)

increases as the beam speed. Thus, in accelerating from 2 to 4 MV, a 1.1 Amp carbon beam will increase to 1.6 Amps. Figure 2 shows operating lines for both constant current and constant bunch length operation. The occupancy is the fraction of the lattice period occupied by the electrostatic quadrupoles. The aspect is the ratio of the lattice length to the clear aperture. The calculations are done for a beam that, at maximum size, fills 2/3 of the clear aperture.

Figure 3 shows the operating characteristics of the magnetically focused portion of the accelerator as a function of the beam energy for parametric pole tip magnetic fields and phase advance per period. The assumption is that a four to one beam combination occurs between the electrostatically focused and magnetically focused accelerators. Hence the larger currents in the magnetically focused accelerator.

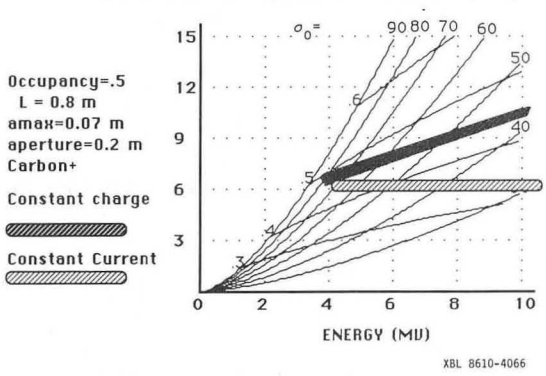

Fig. 3. Operating Characteristics of the magnetically focused accelerator after beam merging. The parametric lines are phase advance per period (σ_0) and magnetic pole tip field in Tesla.

References

1. E.O. Ballard, E.A. Meyer, H. Oona, K.B. Riepe, H.L. Rutkowski, R.P. Shurter, F.W. Van Haaften, D.C. Wilson, S. Humphries, Jr., "Design Status of Heavy Ion Injector Program," Proc. of the Sixth Int. Conf. on High Power Particle Beams, (Kobe, Japan 1986).

STUDIES OF COMBINING BEAMS TRANSVERSELY

David L. Judd

In induction linac systems for inertial fusion ignition, bunch lengths and durations at low energy are large if the number of beams is constant along the linac. Cost considerations favor shorter core pulse times with larger core apertures to contain more beams. Therefore the combining of beams is studied, to produce preliminary conceptual designs, to search for problem areas, to provide cost indications, and to assess technical feasibility. Work thus far has been on combining four beams into one, because design and construction experience with multi-beam systems is for square arrays of sixteen and of four beams.

A system must not make total transverse emittance growth exceeding some small factor, which is not well known because future heavy-ion source systems have unknown emittances and total emittance growth during acceleration is also not well known. Therefore the emittance growth limit is assumed to be small; the combining system should cause the beams to first "see" each other when they are as close as possible, and with their axes as close to parallel as possible.

Before combining, each beam is surrounded by electrostatic or magnetic hardware producing its AG confinement, and a designed clearance space which is hoped to be nearly empty. Each beam must undergo a double bend so that all beams emerge close and parallel. If AG focusing is removed during the double bend, made with fields similar to those in the AG lattice, it has been shown that each beam will roughly double in radius due to its space charge force if it starts at a waist. If it starts doubly converging (due to a special lens system, or "matching section") this might be avoided and a waist produced at the double-bend's end, but the matching section would require an aperture several times that of the upstream AG lattice, which is undesirable. For the cases studied it seems better to provide bending fields in steps, separated by gaps filled with quadrupoles which prevent significant growth in radius or slope.

The transverse spaces between beams, over much of the double-bend region (and certainly its latter half), will be too small to contain the usual AG hardware of the lattice upstream, and also the typical forms of bending-field hardware. For this reason, preliminary studies of pulsed current-sheet dipole and quadrupole four-beam magnet arrays [1] have been made. Such systems, which might require only a very few millimeters space between beams, seem, after first examination by electrical engineers, to represent practical solutions for at least some systems.

Using these concepts, a design [2] was explored for four 1.6-ampere beams of C^{+1} ions at 4 MeV in upstream lattices with $L = 44$ cm, $\sigma_0 = 75°$, $\eta = 2/3$, $\sigma = 12°$, $a_{max} = 2.0$ cm, with axes separated by 8.1 cm. Peak AG fields (from rods) are 3 MV/m. The first bend is made by two 1.3 MV/m fields each of length L/3 separated by a quadrupole like those in the lattice. Following this is an equivalent pulsed-current-sheet quadrupole and a reverse bend of length L/3 by a pulsed magnet at 0.33 T. A final half-quad leads to x and y waists as the beams see one another, 116 cm from the start of the first bend. See Fig. 1, where the bending and focusing regions are shown for one beam, and the four-beam transverse sections at six stations are indicated.

Combining the four beams of the existing MBE-4 induction accelerator system poses a somewhat more difficult design problem, even with the restriction that the four 10-mA beams of Cs^{+1} ions are to be drifted from the 200 keV injector without acceleration. Because of the very low velocity it is more difficult to provide adequate magnetic bending than electric bending, so it seems best to start with a single-segment electric inward bend followed by two (or even three) segments of outward bend, separated by quadrupoles which are electric like the lattice until the necessary space is squeezed out. The magnetic-equivalent pulsed-current-sheet quadrupoles need a rather high field (~ 0.7 T), so a somewhat different design (replacing a continuation of the periodic line) is being considered as work on combining beams is continued.

Studies of beam mixing beyond the double-bend region are being conducted by C. Celata.

References

1. Judd, D.L., "Current-sheet magnetic fields for four-beam merging deflections," HIFAR Note-78, June 1986; "Pulsed current-sheet magnetic quadrupoles," HIFAR Note-79, July 1986.

2. Judd, D.L., "On double bends for beam merging," HIFAR Note-108, July 1986.

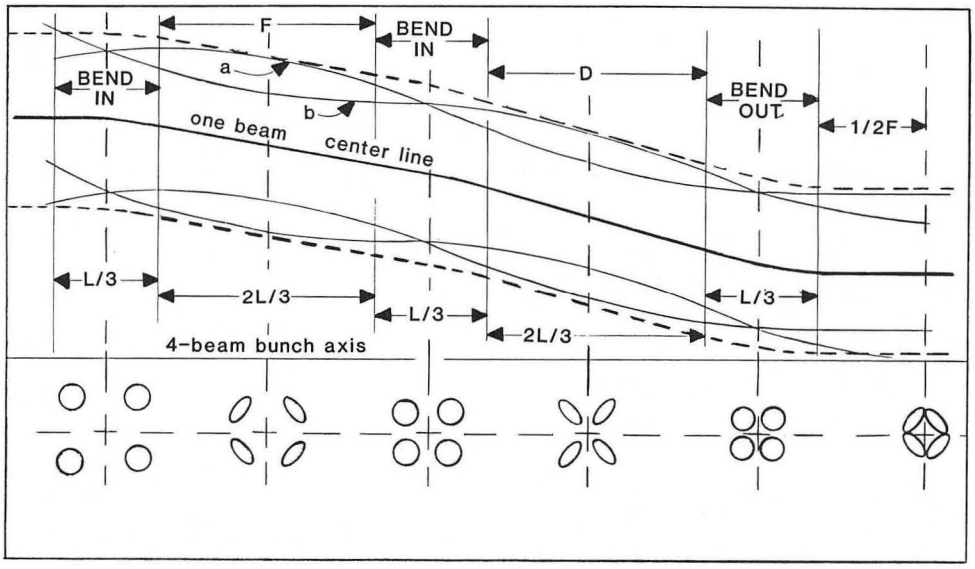

XBL 8611-4313

Fig. 1. Above are shown successive bending and focusing regions, x and y envelopes a and b, for one of the four beams, as described in the text. Below are indicated the transverse sections of all four beams at the six stations shown.

COMPUTER SIMULATION OF TRANSVERSE MIXING OF COMBINED BEAMS

C. M. Celata

In a heavy ion driver it is likely that the most economical accelerator configuration would transport the current in individually focused multiple beams at the low energy end, and would reduce the number of beams by combining at some later stage. It is crucial that the growth in transverse emittance be kept to a minimum during this combining process. This report describes a computer study which calculates the transverse emittance growth when four space-charge-dominated beams which have previously been transported separately emerge into a common AG focusing system and at the same longitudinal location and mix. The system necessary to bring the beams together in this way is described in another report in this collection by David L. Judd.

The transverse combining of 4 identical elliptical uniform beams was studied. The geometry is shown in Fig. 1. Given an initial emittance per beam in the x direction of ε_{ix}, and a final emittance of ε for the combined beam, the emittance growth can be written as

$$\frac{\varepsilon_{fx}}{2\varepsilon_{ix}} = \left(\frac{\varepsilon_{ox}}{2\varepsilon_{ix}}\right)\left(\frac{\varepsilon_{fx}}{\varepsilon_{ox}}\right), \qquad (1)$$

where ε_{ox} is the emittance of the 4 beam initial configuration, shown in Fig. 1. The first factor in Eq. (1) is the "geometrical" emittance dilution which occurs due to the fact that there are empty spaces in the beam. This is a single particle effect which would occur for low intensity beams. The second factor is emittance growth due to the conversion of electrostatic field energy to kinetic energy, plus any growth due to mismatch.

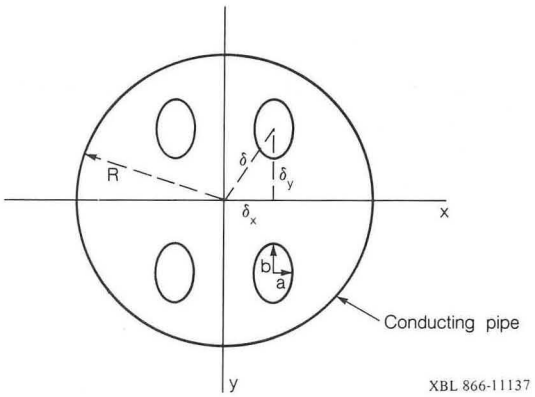

Fig. 1. Transverse plane geometry showing four beams when they first "see" each other.

We will assume below that the initial state has been rms matched, i.e., $\langle x^2\rangle$ and $\langle y^2\rangle$ are periodic solutions of the rms envelope equation. Since the distribution function changes in time, it is not necessarily true that the beam will stay matched throughout the mixing process. Simulation results show that unless the beams are essentially touching, a mismatch results and some beam loss occurs. Both effects increase as the initial distance between beams is increased. In the simulation calculations presented below, the effect of mismatch did not measurably affect transverse emittance growth.

For round beams (i.e., a = b) with $\delta_x = \delta_y$ in a constant focusing system, one can analytically calculate the emittance growth which accompanies the transformation of the configuration of Fig. 1 to a uniform beam with the same (matched) rms radius. This final state is shown by simulation to be the state the beam attains unless there is a substantial mismatch. Conservation of energy gives

$$\frac{\varepsilon_{fx}}{\varepsilon_{ox}} = \sqrt{1 + \frac{|\Delta U|}{K_i}} \qquad (2)$$

where K_i is the total initial transverse kinetic energy per unit longitudinal length, and ΔU is the change in electrostatic field energy per unit length. ΔU is given by

$$\Delta U = \frac{N^2q^2}{16}\left[3 - 4\left[\ln\left(\frac{1-(\delta/R)^8}{4}\right)\right]\left(\frac{a}{\delta}\right)^3\left(1 + \frac{2\delta^2}{a^2}\right)^2\right] \qquad (3)$$

where N is the number of particles per unit length, and q is the charge per particle. The results of the simulation are found to agree with Eqs. (2) and (3), thus confirming that the beam does become uniform. Equation (3) indicates that ΔU is a monotonically increasing function of δ/a, with negligible dependence on δ/R. Therefore if δ/a is kept constant while K_i is increased, the emittance growth given by Eq. (2) will decrease. This can be done by compressing the beams before combining, thus creating hotter beams. The change in transverse momentum is then a smaller fraction of the total, and therefore the relative emittance growth is smaller. Unfortunately, to compress the beams requires first expanding them, which may not be possible within the limited aperture given to each beam. Also, the focusing strength to hold the smaller beam may not be available.

Combining of elliptical beams in an AG focusing system was also explored. The original beams were assumed to have $\sigma_o = 60°$ and $\sigma = 20°$. They were combined at the center of a focusing lens, with the rms radii of the combined beam rms matched for the focusing system ($\sigma_o = 60°$). δ_x and $\xi \equiv (\delta_x/a)/(\delta_y/b)$ were varied. For a given ξ, as δ_x increased, the beam was compressed (before combining) to retain the correct matched radii. The results are shown in Fig. 2. For small δ_x/a the geometrical and space charge contributions to emittance growth were comparable. For larger δ_x/a, where the beams are compressed, the contribution of space charge was much smaller than the geometrical increase. These results show that the total emittance growth in each plane can be kept to about a factor of 2 for the expected values of δ_x/a, so that transverse beam combining can probably be done a number of times in a driver, without compromising the ability to focus the beams on the target.

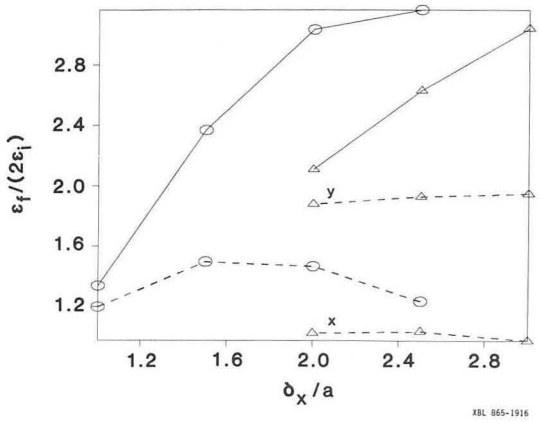

Fig. 2. One-dimensional rms emittance growth vs. δ_x/a for $\xi = 1$ and $\xi = 2$, computed by SHIFTXY. Circles and triangles are simulation results for $\xi = 1$ and $\xi = 2$ respectively. Solid lines are total emittance growth in one plane, $\varepsilon_f/(2\varepsilon_i)$, while dashed lines are the space charge dilution factor only.

ANALYSIS OF THE LOW VOLTAGE REGION OF AN HIF DRIVER

J. Hovingh and E.P. Lee

Introduction

The LBL computer code LIACEP (Linear Induction Accelerator Cost Evaluation Program) was initially written for the high voltage (> 50 MV) region of the linear induction accelerator portion of a HIF driver. The transport featured FODO superconducting magnetic focussing lattices. Later, a module design subroutine was added to LIACEP that utilized electrostatic focussing, with the electrostatic quadrupoles consisting of cantilevered electrodes. Then an electrostatic focussing option using electrodes supported on both ends in a quadrupole array was added to LIACEP as a specified option in the electrostatic focussing module design subroutine. These electrostatic focussing systems are found to be cost effective in the low voltage region (> 50 MV) of the accelerator.

Modification to LIACEP

LIACEP has been modified to compare the costs of both magnetic and electrostatic focussing systems within the code. The costs of both electrode support types are also compared within the code. The code then selects the minimum cost option as the driver design.

Several runs of this modified code have demonstrated substantial cost savings per volt increment using electrostatic focussing in the low voltage region of an accelerator. However, constraints within the electrostatic focussing module design subroutine limit the current to less than that allowed in the module designs using magnetic focussing. We are identifying and attempting to relax these constraints to allow the use of higher currents.

LIACEP and ILSE

The code LIACEP is being used to analyze the design of ILSE, the Induction Linac Systems Experiment. Several LIACEP calculations have been performed using the ILSE preliminary design parameters. LIACEP is not being used to determine a minimum cost ILSE because the cost algorithms in LIACEP assume a mature HIF driver scenario, not a one-of-a-kind experimental facility. The purpose of these LIACEP calculations is to examine the design constraints in LIACEP and aid in the design of ILSE. The module designs used in LIACEP can assist the design of the accelerating modules in ILSE, and the improvements in module design in ILSE can be incorporated, if appropriate for a HIF driver, into LIACEP. Thus, by these iterative processes, we can improve both LIACEP and ILSE.

Improvements to LIACEP

We have identified several deficiencies in LIACEP that are necessary to correct to obtain a more realistic design. We do not currently include a velocity tilt constraint, which is especially important for short pulses in the low voltage region of the accelerator. We also have an inadequate clearance for the beam in the high voltage region. These improvements will be incorporated into LIACEP. Another improvement that will be made to LIACEP is to scan, within the program, a range of depressed tunes for the minimum cost configuration at each voltage. Currently we are doing this by making many runs at different depressed tunes. Figure 1 gives the LIACEP computed current vs. depressed tune (σ) in ILSA for a fixed value of the normalized emittance. The clear trend $I \propto \sigma^{-1}$ holds to very low σ with the assumed parameters, but an ultimate limit is $I \lesssim 2\text{-}3$ amperes, due to an imposed pole tip voltage of ≈100 kV.

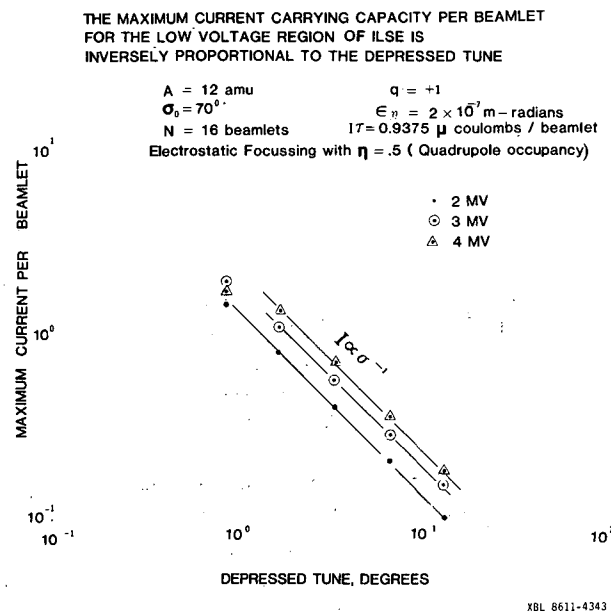

Fig. 1. Transportable Current vs. Depressed Tune in ILSE.

Conclusion

LIACEP is being continually improved to realistically portray the accelerator for a conceptual HIF driver. The interaction of the use of LIACEP with the design of ILSE will improve both LIACEP and ILSE. Further improvements in LIACEP have been identified, and are being incorporated into the program.

PUBLICATIONS AND INTERNAL NOTES

HI-FAN Notes

HI-FAN-308 LBL-21345	D. Keefe	Experiments and Prospects for Induction Linac Drivers Proceedings of the International Symposium on Heavy Ion Fusion, May 27-29, 1986, Washington, D.C.
HI-FAN-314 LBL-21346	E.P. Lee	Accelerator and Final Focus Model for an Induction Linac Based HIF System Study Proceedings of the International Symposium on Heavy Ion Fusion, May 27-29, 1986, Washington, D.C.
HI-FAN-315 LBL-21347	D.L. Judd C.H. Kim L.J. Laslett L. Smith A.I. Warwick	Head-to-Tail Velocity Tilt in an Ion Induction Linac Proceedings of the International Symposium on Heavy Ion Fusion, May 27-29, 1986, Washington, D.C.
HI-FAN-316 LBL-21348	T.J. Fessenden D.L. Judd D. Keefe C. Kim L.J. Laslett L. Smith A.I. Warwick	Preliminary Results from MBE-4: A Four Beam Induction Linac for Heavy Ion Fusion Research Proceedings of the International Symposium on Heavy Ion Fusion, May 27-29, 1986, Washington, D.C.
HI-FAN-317 LBL-21349	C.M. Celata	Simulation of Transverse Merging of Space-Charge-Dominated Beams Proceedings of the International Symposium on Heavy Ion Fusion, May 27-29, 1986, Washington, D.C.
HI-FAN-318 LBL-21350	J. Hovingh E.P. Lee A. Faltens V.O. Brady	The Cost of Induction Linac Drivers for Inertial Fusion for Various Target Yields Proceedings of the International Symposium on Heavy Ion Fusion, May 27-29, 1986, Washington, D.C.
HIFAN-319 LBL-20979	J. Hovingh V.O. Brady A. Faltens E.P. Lee	A Comparison of the Design and Costs of Induction Linac Drivers for Inertial Fusion Using Ions of Differing Mass. Presented at the 1986 Annual Meeting of the American Nuclear Society, Reno, NV, June 15-19, 1986.

HI-FAN-320 LBL-21559	E.P. Lee	Transport of Intense Ion Beams To be published in the Proceedings of the Second International Conference on Charged Particle Optics, May 19-23, 1986
HI-FAN-321 LBL-21194	T.J. Fessenden C.M. Celata A. Faltens T. Henderson D.L. Judd D. Keefe L.J. Laslett J. Meneghetti C. Pike D. Vanecek	Preliminary Design of A 10 MV Ion Accelerator for HIF Research Presented at the Second International Topical Symposium on ICF Research by Particle Particle Beams, Nagaoka, Japan, June 16-18, 1986.
HI-FAN-322 LBL-21744	T.J. Fessenden R.T. Avery D.A. Brodzik C.S. Chavis A. Faltens D.E. Gough T.F. Henderson D.L. Judd D. Keefe C. Kim L.J. Laslett J.R. Meneghetti C.D. Pike L. Smith D.L. Vanecek A.I. Warwick	MBE-4: An Induction Linac Experiment for Heavy Ion Fusion Presented at the Sixth International Topical Conference on High-Power Electron and Ion-Beam Research and Technology, Kobe, Japan, June 9-12, 1986
HI-FAN-323 LBL-21745	Denis Keefe	Highlights of the Heavy Ion Fusion Symposium Presented at the LINAC 86 Conference, SLAC, Stanford, CA, June 2-6, 1986
HI-FAN-324 LBL-21527	Denis Keefe	Advanced Concepts for Acceleration Presented at High-Brightness Accelerators, Pitlochry (Perthshire), Scotland, July 13-25, 1986
HI-FAN-325 LBL-21528	Denis Keefe	Induction Linacs To be presented at the High-Brightness Accelerators, Pitlochry (Pertshire), Scotland, July 13-25, 1986
HI-FAN-326 LBL-21854	C.M. Celata C.H. Kim MFE Group	Abstracts submitted for the 28th Annual Meeting, Division of Plasma Physics, Nov. 3-7, 1986

HI-FAN-327 LBL-21758	D.E. Gough D.A. Brodzik	Pulser Development for MBE-4 Presented at the 1986 Seventeenth Power Modulator Symposium, Seattle, Washington, June 23-25, 1986
HI-FAN-328	J. Hovingh V.O. Brady A. Faltens E.P. Lee	A Comparison of the Design and Costs of Induction Linac Drivers for Inertial Fusion Using Ions of Mass 133 and 200. (7/86)
HI-FAN-329	T. Fessenden et. al	Vugraphs for JASON HIFAR Review June 16, 1986
HI-FAN-330	T. Fessenden	Foreign Travel Report/Japan, June 9-12.
HI-FAN-331 LBL-21969a	D. Keefe	Review of Progress in the U.S. Heavy Ion Fusion Program To be presented at APS Meeting in Baltimore, Md. November 3-7, 1986 (invited paper).
HI-FAN-332 LBL-21826	J. Hovingh V.O. Brady A. Faltens E.P. Lee	A Comparison of the Design and Costs of Induction Linac Drivers for Inertial Fusion Using Ions of Mass 133 and 200 Presented at the Seventh Topical Meeting on the Technology of Fusion Energy, Reno, Nevada, June 15-19, 1986
HI-FAN-333 LBL-22415	Denis Keefe	Linear Accelerators for Heavy Ion Fusion To be presented at the High-Brightness Accelerators, Pitlochry (Pertshire), Scotland, July 13-25, 1986
HI-FAN-334	J.W-K. Mark	Approaching Maximal Performance of Longitudinal Beam Compression in Induction Accelerator Drivers
HI-FAN-335	D. Keefe	Heavy Ion Fusion Accelerator Research Program BES Briefing, September 8, 1986. (9/30/86).
HI-FAN-336 LBL-22276	C. Celata A. Faltens T.J. Fessenden D.L. Judd D. Keefe C.H. Kim L.J. Laslett E.P. Lee M.G. Tiefenback L. Smith A.I. Warwick	Research in the U.S. on Heavy Ion Drivers for Inertial Confinement Fusion. To be published in the Proceedings of the IAEA 11th International Conference on Plasma Physics and Controlled Nuclear Fusion Research, Kyoto, Japan, Nov. 13-20, 1986

HI-FAN-337	V. Brady	Computational Analysis of a Permanent Magnet Quadrupole
HI-FAN-338	E. P. Lee E. Close L. Smith J. Kalnins A. Faltens D. Shuman	Poster from NPB Meeting at LANL (10/02/86)
HI-FAN-339 LBID-1216	M. Cornacchia S. Chattopadhyay A. Garren E.P. Lee	Foreign Trip Report
HI-FAN-340 PUB-5178	HIF Staff	Heavy Ion Fusion Accelerator Research: An Outline Plan (September 1986)
HI-FAN-341 LBL-22211a	C.M. Celata A. Faltens David L. Judd L. Smith M.G. Tiefenback	Transverse Combining of Nonrelativistic Beams in a Multiple Beam Induction Linac Abstract submitted to the 1987 Particle Accelerator Conference, March 16-19, 1987 Washington, D.C.
HI-FAN-342 LBL-22214a	C.M. Celata	Transverse Dynamics of Space-Charge-Dominated-Ion Beams Invited abstract submitted to the 1987 Particle Accelerator Conference, March 16-19, 1987, Washington, D.C.
HI-FAN-343 LBL-22215a	J. Kalnins C.M. Celata L. Smith	Emittance Growth of an Intense Ion Beam Due to an Initial Mismatch Abstract submitted to the 1987 Particle Accelerator Conference, March 16-19, 1987, Washington, D.C.
HI-FAN-344 LBL-22216a	E.P. Lee E. Close L. Smith	Space Charge Effects in a Bending Magnet System Abstract submitted to the 1987 Particle Accelerator Conference, March 16-19, 1987, Washington, D.C.
HI-FAN-345 LBL-22217a	T.J. Fessenden D. Keefe C.H. Kim A.I. Warwick	The LBL Multiple Beam Experiments Invited abstract submitted to the 1987 Particle Conference, March 16-19, 1987 Washington, D.C.
HI-FAN-346 LBL-22272a	C.H. Kim	Pulse Shaping in an Ion Induction Linac Abstract submitted to the 1987 Particle Accelerator Conference, March 16-19, 1987, Washington, D.C.

HI-FAN-347 LBL-22274a	D. Gough D. Brodzik A. Faltens C. Pike J. Stoker	Pulsers for the Induction Linac MBE-4 Abstract submitted to the 1987 Particle Accelerator Conference, March 16-19, 1987 Washington, D.C.
HI-FAN-348 LBL-22275a	M.G. Tiefenback	Emittance Growth in Mismatched Space-Charge-Dominated Beams Abstract submitted to the 1987 Particle Accelerator Conference, March 16-19, 1987, Washington, D.C.
HI-FAN-349 LBL-22411	D. Keefe	Prospects for Fusion Power To be published in the Journal of Fusion Energy

HIFAR Notes (Internal and Informal)

HIFAR-Note-60	C. Pike J. Stoker	MBE-4 Insulator Tests. (4/86)
HIFAR-Note-61	J. Hovingh	Economic Aspects of Beam Merging with Changes in Emittance and Depressed Tune in 4.25 MJ HIF Driver at Voltages above 50 MV. (4/86)
HIFAR-Note-62	J. Laslett	Values of Q/U^2 in the Asymptotic Limit 4/21/86
HIFAR-Note-63	J. Laslett	Values of Q/u^2 vs σ/σ_0 4/21/86
HIFAR-Note-64	J. Laslett	Transport, at Injection, of Charged-State 3 vs Charge State 1. (4/21/86)
HIFAR-Note-65	D. Brodzik	Preliminary Tests - 4" Silicon Steel Cores (MAR-JAN SILICON STEEL, 3%). 4/86
HIFAR-Note-66	L. Smith	Frequency Response of Beam to High Frequency Voltage Errors in Accelerating Modules (4/30/86)
HIFAR-Note-67	C. Kim	A Possible MBE-4 Configuration Using MAR-JAN Cores/Pulsers. (4/3/86)
HIFAR Note-68	D. Brodzik	MBE-4 SEC A and B (Core and PFN Database) 4/30/86
HIFAR Note-69	D.L. Judd	On Enclosing N Identical Ellipses by a Single Ellipse with Minimum Excess Included Area. (4/6/86)
HIFAR Note-70	D. L. Judd	Simple General Derivation of the Familiar Approximate Relation for Head-To-Tail Velocity Tilt. (4/4/86)
HIFAR Note -71	D.L. Judd	Rough Estimates of Some Effects of Proposed Waveform Shapes in MBE-4 Sec. C. (2/20/86)
HIFAR Note-72	J. Laslett A. Faltens	Revised Tune Prescriptions. (4/25/86)
HIFAR Note-73	D. Brodzik	SEC C Cores and pulse Capabilities (5/15/86)
HIFAR Note-74	L. Smith	Effect of Quadrupole Azimuthal Errors (5/16/86)

HIFAR Note-75	A. Faltens	Black and White Clouds and Their Relation to Multiple Pulsing and Beam Merging. (5/86)
HIFAR Note-76	C. Pike G. Stoker	MBE-4 Quad Insulators - Voltage holding after exposure to beam
HIFAR Note-77	T. Warwick	Hardware Required for Emittance Measurements on MBE-4. (6/17/86)
HIFAR Note-78	D. Judd	Current-Sheet Magnetic Fields for Four-Beam Merging Deflections. (6/27/86)
HIFAR Note-79	D. Judd	Pulsed Current-Sheet Magnetic Quadrupoles July 1986
HIFAR Note-80	L.J. Laslett	Additional Tables of Q/u^2 in The Asymptotic Limit. July 1986
HIFAR Note-81	L.J. Laslett	A Periodic Quadrupole Lattice Formed from Permanent Magnets July 1986
HIFAR Note-82	L.J. Laslett	The Use of Permanent Magnets to excite the Iron Poles of a Periodic Quadrupole Array July 1986
HIFAR Note-83	L.J. Laslett	An Iron-Free Current Configuration for Production of a Periodic Quadrupole Array July 1986
HIFAR Note-84	L.J. Laslett	A Second Iron-Free Current Configuration for Production of a Periodic Quadrupole Lattice July 1986
HIFAR Note-85	T. Fessenden C. Pike	Some Cost/Budget Options for ILSE July 22, 1986.
HIFAR Note-86	L.J. Laslett	ISLE Design -- Transverse Focusing Specifically 2 MV to 4 MV Region Flexible Options. (7/86)
HIFAR Note-87	J. Stoker R. Hipple	Gradent Rings for 85% Alumina and Stratite MBE-4 Quadrapole Insulators. (7/86)
HIFAR Note-88	T. Fessenden M. Tiefenback	Future Single Beam Transport Experiments
HIFAR Note-89	D.E. Gough	Pulsers for MBE-4 Section C. August 6, 1986
HIFAR Note-90	M. Tiefenback	Slit Alignment Effects in the SBTE August 12, 1986

HIFAR Note-91	A. Faltens J. Stoker	The Ford Pulser Tests. August 14, 1986
HIFAR Note-92	M. Tiefenback	Due to Mismatching of Space-Charge-Dominated Beams. August 18, 1986
HIFAR Note-93	J. Hovingh	LIACEP Analysis of Selected HIFSA Systems Code Sampel Cases. August 19, 1986
HIFAR Note-94	J. Hovingh	Cost Analysis of ILSE Using LIACEP. (8/20/86)
HIFAR Note-95	A. Faltens	An Alternate MBE Scenario. (8/22/86)
HIFAR Note-96	D. Vanecek	Accelerator Section "C D E F" - Core Detail August 14, 1986.
HIFAR Note-97	A. Faltens	Core Packaging Options. (9/11/86)
HIFAR Note-98	L. Smith	Longitudinal Perturbation af a Cold Beam. September 17, 1986
HIFAR Note-99	C. Pike R. Hipple G. Stoker	Modification of Quadrupole Insulators (9/30/86)
HIFAR Note-100	A. Faltens	Double Pulsing Experiments. (9/4/86)
HIFAR Note-101	C. Kim	Voltage Waveforms for MBE-4 Sections C and D. (9/29/86).
HIFAR Note-102	J. Hovingh	Note to Denis Keefe regarding transport equations in LIACEP
HIFAR Note-103	C. Pike R. Hipple G. Stoker D. Vanecek	Quadrupole Feed-Thru Insulator Tests (9/25/86)

H.I.F. STAFF ROSTER

Denis Keefe

Robert T. Avery
Donald A. Brodzik
Clarence Chavis
Warren Chupp
Andris Faltens
Thomas J. Fessenden
Bill Ghiorso
David Gough
Wayne Greenway
Edward C. Hartwig
T. Henderson
Ralph Hipple
Cai Houston
Gilbert Jones
Charles H. Kim
Bruce MacDonell
John Meneghetti
Harry Meyer
Chester D. Pike
Tom Purtell
Jim Rice
Stuart Ryce
Gerald L. Stoker
Michael Tiefenback
Bill Tiffany
Mike Towler
David Vanecek
Anthony Warwick

Lloyd Smith

Victor Brady
Christine Celata
David L. Judd
L. Jackson Laslett
Edward P. Lee

William B. Herrmannsfeldt, SLAC

Jack Hovingh, LLNL

HALF-YEAR/YEAR-END REPORT: DISTRIBUTION LIST

Allied Chemical Corporation

Carl Smith

Argonne National Lab.

Thomas A. Fields
Ronald Martin

University of Arizona

R. Morse

Batelle

John Hartman

Bechtel

W. Allen

BMD/ATC/SDC

Milton Hawie
Brian Strickland

Brookhaven National Lab.

Mark Barton
E. Courant

C.E.A. Bruyeres-le-Chatel

R. Dei-Cas

CEBAF

J. Bisognano
D. Douglas
H. Grunder
G. Krafft
C. Leemann

University of Calif., Irvine

Norman Rostoker

Cornell University

John Nation
Ravi N. Sudan

DARPA

H. Lee Buchanan

Department of Defense (SDIO)

Richard Gullickson
Alan Mense

Department of Energy

DP-OIF

Gregory D'Alessio
Sheldon L. Kahalas
R. Schriever
Marshall Sluyter

ER

Ryszard Gajewski (AEP)
Terry Godlove (AEP)
Gerry Peters (HENP)
W. Polansky (AEP)
Robert Rader (OPA)
D. Stevens (BES)
David F. Sutter (HENP)
Alvin Trivelpiece, Dir.,
Office of Energy Research
William Wallenmeyer (HENP)

DoE San Office

Rudolf Bredderman
Dennis Neely

E.P.R.I.

Robert Scott

Fermi National Accelerator Lab.

Frank T. Cole
Fred Mills
Lee Teng

F.O.M. Amsterdam

F. Siebenlist

GANIL

P. Lapostolle

GE

John Lucek

GSI

R. Bock
D. Boehne
I. Hofmann
A. Warwick

University of Illinois

G. Miley

Institute for Nuclear Study

Y. Hirao

KMS Fusion, Inc.

Alex Glass

Kanazawa University

S. Kawasaki

Lawrence Berkeley Laboratory

D. Atwood, 80/101
R. Avery, 46/189
K. Berkner, 50/149
D. Brodzik, 46/125
C. Celata, 47/112
W.W. Chupp, 47/112
M. Cornacchia, 47/112
T. Elioff, 90/4040
A. Faltens, 47/112
T. Fessenden, 47/112
A. Garren, 47/112
D. Gough, 47/112
E. Hartwig, 47/112
H. Heckman, 50/245
T. Henderson, 46/161
E. Hoyer, 46/187
E. Hyde, 50A/4133E
R. Johnson, 50A/4119
D. Judd, 47/112
G. Kalnins, 47/112
D. Keefe, 47/112
C. Kim, 47/112
M. Krebs, 50A/4112
W. Kunkel, 4/230
G. Lambertson, 47/112
L.J. Laslett, 47/112
E.P. Lee, 47/112
E. Lofgren, 47/112
J. Marx, 50/149
J. Meneghetti, 46/161
J. Peterson, 90/4040
A. Sessler, 4/230
D. Shirley, 50A/4133
L. Smith, 47/112
C. Taylor, 46/161
D. Vanecek, 58/1011
D. Vaughan, 50/149

Lawrence Livermore Laboratory

Roger Bangerter, L-477
W. Barletta, L-626
Richard J. Briggs, L-321
John L. Emmett, L-488
Darwin Ho, L-477
John Holzrichter, L-481
William Krupke, L-488
J. Lindl, L-477
Jim Mark, L-477
John Nuckolls, L-477

Lawrence Livermore Laboratory (cont'd)

Louis Reginato, L-526
Erik Storm, L-481

Lockheed

John Siambis

Los Alamos National Laboratory

Ihor Bohachevsky
Richard Cooper
Robert Jameson
Tom MacDonald
Earl Meyer
Roger B. Perkins
Richard Stokes
Tai-Sen Wang
Doug Wilson

University of Maryland

Martin Reiser
Derek Tidman

Max Planck Inst. fur
Plasma Physik Garching

Arnulf Schluter

Maxwell Laboratories

Library

National Bureau of Standards

S. Penner
M. Wilson

Naval Research Lab.

Steven Bodner
T. Coffey
Irving Haber
Philip Sprangle
Peter Turchi

Occidental Research Corp.

Wyn Salisbury

Osaka University

T. Mochizuki
C. Yamanaka

Universita di Padova

A. Pascolini
M. Pusterla

Physical Dynamics

G. H. Gillespie

Physics International

Library

Pulse Sciences, Inc.

Ian Smith
Kurt Nielson
M. Tiefenback

RAFAEL

Joseph Shiloh

Rutherford Laboratory

John D. Lawson
Chris Pryor
Graham Rees

Sandia Laboratories

Everet H. Beckner
Don Cook
Glenn Kuswa
Tom Martin
J.P. VanDevender

W.J. Schafer Associates

Michael J. Monsler

SLAC

William Herrmannsfeldt, Bin 26
Burton Richter, Bin 7

Soka University

Tetsuya Saito

SOREQ Nuclear Research Center

A. Sternlieb

TITAN Systems

Ken Billman
G. Yonas

TRW

J. Gordon
Z. Guiragossian
J. Maniscalco
A.W. Maschke
W. Steele

UCLA

John Dawson

University of Texas at Austin

Toshi Tajima

URA

Edward Knapp

Varian

S.S. Rosenblum

Westinghouse

M. Nahemow
E. W. Sucov

University of Wisconsin

G. Kulcinski
G. Moses
R. Peterson

This report was done with support from the Department of Energy. Any conclusions or opinions expressed in this report represent solely those of the author(s) and not necessarily those of The Regents of the University of California, the Lawrence Berkeley Laboratory or the Department of Energy.

Reference to a company or product name does not imply approval or recommendation of the product by the University of California or the U.S. Department of Energy to the exclusion of others that may be suitable.

LAWRENCE BERKELEY LABORATORY
TECHNICAL INFORMATION DEPARTMENT
UNIVERSITY OF CALIFORNIA
BERKELEY, CALIFORNIA 94720